To appear in *Space Physics and Aeronomy, Volume 4: Upper Atmosphere Dynamics and Energetics* (AGU Geophysical Monograph Series), edited by W. Wang and Y. Zhang

Joule Heating in the Thermosphere

A. D. Richmond[1]

[1] High Altitude Observatory, National Center for Atmospheric Research, 3080 Center Green Drive, Boulder, CO 80301, USA.

Corresponding author: Arthur D. Richmond (richmond@ucar.edu)

Key Points:

- Joule heating by currents from the magnetosphere has a highly variable impact on thermospheric properties
- Winds and structures in the electric conductivities, fields, and currents have important impacts on Joule heating
- Heating-induced gravity waves and circulation changes strongly affect the thermospheric density and composition response

Abstract

High-latitude Joule heating is an important energy source for thermospheric dynamics and composition. It is influenced by winds, plasma turbulence, variable electric fields, and conductivity modifications by strong electric fields. The height-integrated heating can be estimated from the Poynting flux above the ionosphere. Most energy is deposited near the morning and afternoon/evening sides of the auroral oval and in the cusp region. Multi-instrument data assimilation can help quantify complex spatial/temporal variations of Joule heating. Rapid changes of heating launch gravity waves that propagate globally. Within several hours a global circulation sets up that reduces horizontal variations of the pressure scale height, causing spatial correlation between the temperature and the mean molecular mass. The distributions of temperature and density in the upper thermosphere often show little relation to the distribution of Joule heating. Vertical winds decrease the O/N_2 ratio in regions of heating and increase the ratio in regions of subsidence. The upper thermosphere is affected more strongly by the fraction of Joule heating deposited above 150 km than by the larger amount of Joule heating deposited below 150 km.

Plain Language Summary

Electric currents from the magnetosphere are an important and highly variable source of heat for the high-latitude upper atmosphere. The heating depends not only on the large-scale electric fields and currents, but also on winds and on small- and medium-scale variable structures in the fields and currents. The heating is strongest at auroral latitudes. Observations from many different instruments in space and on the ground can be combined to estimate the heating. The atmosphere responds to the heating with waves that propagate globally and with winds that change the three-dimensional global circulation within several hours after the heating changes. The circulation affects the upper atmospheric temperature, composition, and density in complex ways. The atmospheric responses are sensitive to the altitude where heating occurs and to the duration of the heating.

1 Introduction

Joule heating, which is the irreversible conversion of electromagnetic energy into heat through ohmic currents, is a significant source of energy for the high-latitude thermosphere (Cole, 1962; Thayer, 2000; G. Lu et al., 2016). Unlike heating by solar ultraviolet and extreme ultraviolet radiation, Joule heating occurs over only a small fraction of the Earth, and can drive large vertical velocities that alter the thermospheric circulation, leading to local and global temperature increases and changes in the structure of thermospheric composition, temperature, and density (e.g., Taeusch et al., 1971; Mayr & Volland, 1972, 1973; Mayr et al., 1978; Volland, 1979; Roble et al., 1983; Rees & Fuller-Rowell, 1989; Rees, 1995; H. Liu & Lühr, 2005; Sutton et al., 2005; Lei et al., 2010; R. Liu et al., 2010; Fedrizzi et al., 2012; Fuller-Rowell, 2013). Thermospheric responses to Joule heating during magnetic storms can be dramatic (e.g., Prölss, 1980, 1995; Rishbeth, 1991; Fuller-Rowell et al., 1994, 1997; Rees, 1995; G. Lu et al., 2016; Deng et al., 2018). In addition to temperature increases, which produce large density increases in the upper thermosphere, the upwelling in the high-latitude region of heating induces a global circulation within several hours (Volland & Mayr, 1971; Mayr & Volland, 1973), accompanied by downwelling at lower latitudes. The circulation dampens the upper-thermosphere density response at high latitudes and spreads this response globally. The upwelling decreases the O/N_2 ratio at high latitudes (Taeusch et al., 1971; Mayr & Volland, 1972; G. Lu et al., 2016). Rapid variations of the heating generate thermospheric gravity waves in the lower thermosphere that propagate globally into the upper thermosphere, causing oscillations of wind, temperature, composition, and density as well as large-scale traveling ionospheric disturbances (e.g., Wright, 1960; G. Lu et al., 2016). The effects of Joule heating depend not only on its highly variable intensity and its distribution over the polar regions, but also depend on the altitude distribution of the heating. Effects observed in the upper thermosphere have a complex relation to the heating distribution, such that thermospheric density increases usually do not coincide with regions of maximum heat input, due not only to the presence of gravity waves, but also to the fact that circulation changes rapidly redistribute density (Johnson, 1960). Furthermore, temperature changes are coupled to composition changes, such that the temperature and the thermospheric O/N_2 ratio tend to be inversely correlated in space. This is due to the tendency of the circulation to smooth out horizontal variations of the pressure scale height (Hays et al., 1973). This effect contributes to the fact that horizontal variations of density and composition during magnetic storms can be very different (e.g., Lei et al., 2010).

2 Physics of Joule heating

The physics of thermospheric Joule heating involves collisional interactions among electrons, positive ions, and neutral molecules. These species have differential bulk motions owing to the presence of electric and magnetic fields, so that collisions result in frictional momentum exchange and heating (e.g., Brekke & Kamide, 1996; Thayer & Semeter, 2004; X. Zhu et al., 2005; Vasyliunas & Song, 2005; Strangeway, 2012). The sum of frictional heating of all species gives the total Joule heating. The frictional heating causes the species to have different temperatures, with the electron and ion temperatures exceeding the neutral temperature (e.g., St. Maurice & Hanson, 1982; Heelis & Coley, 1988; St. Maurice et al., 1999), and additional collisions transfer heat from hotter to cooler species. On time scales longer than the heat-transfer times between ions and neutrals and between electrons and ions, and neglecting heat loss through conduction, radiation, or chemistry, a quasi-steady state is reached in which the heat is shared among the species in proportion to their number densities and particle degrees of freedom (three degrees of freedom for each particle plus two internal degrees of freedom for molecules), multiplied by their respective temperatures. Because the number density of neutral particles greatly exceeds the density of ions and electrons, almost all of the heat ends up residing in the neutral component of the gas.

For quasi-steady-state motions the volumetric total frictional or Joule heating rate is

$$Q = Nm_i\nu_{in}(\mathbf{V}_i - \mathbf{V}_n)^2 + Nm_e\nu_{en}(\mathbf{V}_e - \mathbf{V}_n)^2 + Nm_e\nu_{ei}(\mathbf{V}_e - \mathbf{V}_i)^2 \tag{1}$$

where N is the electron (and ion) number density: m_i and m_e are the ion and electron masses; ν_{in}, ν_{en}, and ν_{ei} are the ion-neutral, electron-neutral, and electron-ion collision frequencies for momentum transfer (assumed here to be isotropic); and $\mathbf{V}_i$, $\mathbf{V}_n$, and $\mathbf{V}_e$ are the ion, neutral, and electron bulk velocities. Because $m_i\nu_{in}$ is much larger than $m_e\nu_{en}$ and $m_e\nu_{ei}$, ion-neutral collisions usually dominate Joule heating, except sometimes at low altitudes where these collisions cause the ion-neutral velocity difference ($\mathbf{V}_i - \mathbf{V}_n$) to become very small. Electron-neutral collisions become important in the lower E-region ionosphere, where Joule heating is relatively small except where strong turbulent electric fields can be present (see Section 4). The contribution of electron-ion collisions to total Joule heating is insignificant.

By solving the momentum equations for ions and electrons to get their velocities in terms of the neutral wind $\mathbf{V}_n$ and the electric field components $\mathbf{E}_\perp$ and $\mathbf{E}_\parallel$ perpendicular and parallel to the geomagnetic field $\mathbf{B}$ (ignoring the small gravitational and pressure-gradient forces on the plasma) we can obtain Ohm's Law for the current density $\mathbf{J}$:

$$\mathbf{J} = Ne(\mathbf{V}_i - \mathbf{V}_e) = \sigma_P (\mathbf{E}_\perp + \mathbf{V}_n \times \mathbf{B}) + \sigma_H\, \mathbf{b} \times (\mathbf{E}_\perp + \mathbf{V}_n \times \mathbf{B}) + \sigma_\parallel \mathbf{E}_\parallel \qquad (2)$$

where σ_P, σ_H, and $\sigma_\parallel$ are the Pedersen, Hall, and parallel conductivities and $\mathbf{b}$ is a unit vector along $\mathbf{B}$. In terms of these quantities the total Joule heating rate can also be expressed as

$$Q = \mathbf{J} \cdot (\mathbf{E} + \mathbf{V}_n \times \mathbf{B}) = \sigma_P (\mathbf{E}_\perp + \mathbf{V}_n \times \mathbf{B})^2 + \sigma_\parallel E_\parallel^2. \qquad (3)$$

The total electromagnetic energy transfer rate to the medium is

$$\mathbf{J} \cdot \mathbf{E} = \mathbf{J} \cdot (\mathbf{E} + \mathbf{V}_n \times \mathbf{B}) + \mathbf{V}_n \cdot \mathbf{J} \times \mathbf{B} = Q + \mathbf{V}_n \cdot \mathbf{J} \times \mathbf{B} \qquad (4)$$

where $\mathbf{J}$ is the electric current density. While Q on the right-hand side of (4) is always positive, the second term, representing the rate of work done on the medium by the Ampère force, can be either positive or negative. The work may result in adiabatic changes of bulk kinetic energy, internal energy, and potential energy.

3 Wind effects on Joule heating

When $\mathbf{V}_i - \mathbf{V}_n$ is large enough to produce significant Joule heating, in regions where $N m_i \nu_{in}$ is sufficiently large, it is usually because the magnitude of $\mathbf{V}_i$ becomes much larger than the magnitude of $\mathbf{V}_n$. A rough estimate of Joule heating can be obtained by neglecting $\mathbf{V}_n$ altogether. However, $\mathbf{V}_n$ is often large enough to affect Joule heating substantially (Brekke & Rino, 1978; Thayer & Vickrey, 1992; G. Lu et al., 1995; Thayer et al., 1995; Thayer, 1998, 2000; Fujii et al., 1999; Deng & Ridley, 2007; Aikio et al., 2012; Cai et al., 2013, 2014; Hurd & Larsen, 2016; Billett et al., 2018). Billett et al. (2018) used empirical models of ion convection, wind, and conductivity to show that winds usually increase Joule heating in the dawn-side auroral region, but usually decrease Joule heating in the polar cap and dusk-side auroral region. In the auroral zone E region, Fujii et al. (1999) found that, on the average, winds reduce Joule heating by 35% at 125 km and by 10% at 117 km, but that winds contribute positively to Joule heating at 109 km and 101 km. In the lower thermosphere, Thayer (1998) and Hurd and Larsen (2016) found that height-varying winds have a strong influence on the height structure of Joule heating. Aikio et al. (2012) analyzed the statistics of the height-integrated Joule heating and generation of wind kinetic energy at the EISCAT Tromsø radar between 80 km and 180 km for different magnetic local times (MLTs) and K_p levels, while Cai et al. (2013) analyzed the height variations of these quantities. They found that the wind usually increases Joule heating relative to what it would be with the same electric field and conductivity, although a wind-induced decrease of Joule heating often occurs above 120 km, especially in the afternoon and evening.

It is important to recognize that the wind is not independent of the ion velocity but is strongly influenced by it (e.g., Axford & Hines, 1961; Cole, 1962; Rees, 1971; Rees & Fuller-Rowell, 1991; Fujii et al., 1999). When ion densities are large, as in the sunlit F region, ion drag tends to accelerate the wind toward the ion velocity on time scales ranging roughly from three hours (ion density 10^{11} m^{-3}) down to twenty minutes (ion density 10^{12} m^{-3}), although this ion drag competes with other forces on the air, so that the velocity difference does not disappear. Rees and Fuller-Rowell (1991) pointed out that the reduction of the ion-neutral velocity difference by ion-drag-driven winds means that electric current densities and Joule heating are also reduced. Steady ion velocities have a larger impact than rapidly varying ion velocities, if the latter do not persist long enough to accelerate the air very much. In the upper E region Thayer (1998) found that winds produced by steady electric fields tend to reduce Joule heating, but that winds in the presence of variable electric fields tend to increase Joule heating, on average. In the latter case, the increase of Joule heating at times when $\mathbf{V}_i$ and $\mathbf{V}_n$ are opposed is greater than the reduction of Joule heating at times when $\mathbf{V}_i$ and $\mathbf{V}_n$ are in the same direction, for equal magnitudes of $\mathbf{V}_n$, because of the quadratic relation of Joule heating to the velocity difference, yielding a net increase of Joule heating on average.

4 Effects of irregularities and electric-field variability

When global estimates of Joule heating are needed, studies often use empirical models of electric fields together with conductivities derived from empirical models of solar ionizing radiation and auroral particle precipitation. These models are usually good at representing the average large-scale electric field and conductivity for specific geophysical conditions: magnetic latitude, MLT, season, interplanetary magnetic field (IMF), or other quantities. However, they typically do not represent the variability of electric fields, currents, and conductivities about the average. Variability on spatial scales smaller than the smoothed empirical models can occur on scales ranging from small-scale plasma waves to structures with scale sizes of tens or hundreds of kilometers. The requirement that electric current is essentially continuous everywhere means that irregularities in the conductivity engender irregularities in the electric field to maintain current continuity.

Plasma instabilities produce plasma waves with fractional electron-density fluctuations that can reach 10% or more of the background electron density (e.g., Oppenheim et al., 2008). Because of Hall polarization effects, these electron-density fluctuations can produce small-scale electric fields several times larger than the large-scale background electric field. Moreover, the irregularities tend to produce small-scale electric fields parallel to $\mathbf{B}$ that can be orders of magnitude larger than the average parallel electric field (e.g., St. Maurice & Laher, 1985; Providakes et al., 1988; St. Maurice, 1990; Dimant & Milikh, 2003; Milikh & Dimant, 2003), which can raise the electron temperature significantly (e.g., Bahcivan, 2007). Both the enhanced perpendicular electric field and the strongly enhanced parallel electric field increase the mean Joule heating (e.g., Dimant & Oppenheim, 2011a). Heelis & Vickrey (1991) pointed out that even without irregularities in the plasma density, small-scale irregular structures in the electric field above the ionosphere also affect the strengths of the perpendicular and parallel electric field in the ionosphere below, and therefore affect the Joule heating.

Variance of the perpendicular electric field on scales greater than several kilometers can be comparable to the squared mean field (e.g., Codrescu et al., 1995, 2000; Crowley & Hackert, 2001; Matsuo et al., 2003; Matsuo and Richmond, 2008; Cosgrove and Thayer, 2006; Cosgrove et al., 2011; Hurd & Larsen, 2016), but only part of the observed variance is associated with irregular plasma structures, as opposed to temporal variability of the large-scale electric field. Crowley and Hackert (2001) showed that much of the temporal variability occurs with periods less than one hour. Matsuo and Richmond (2008) analyzed the electric-field variability about the mean model of Weimer (2001) in terms of "resolved" and "subgrid" components, where the "subgrid" component essentially included wavelengths of 8-1000 km along polar passes of the DE-2 satellite. The "subgrid" component is considerably stronger in winter than summer, but has little dependence on the IMF direction. The "resolved" component has less seasonal variation but is notably stronger for southward IMF than other IMF directions. Matsuo and Richmond (2008) found that the thermospheric wind response to the variable electric field depends significantly on its temporal coherence. Cosgrove and Codrescu (2009) discussed how the magnitude of electric-field variability depends on how the mean electric field is defined for particular geophysical conditions. They proposed a way of defining "small-scale" vs. "resolved-scale" electric-field variability, which was used by Cosgrove et al. (2011) to quantify the electric-field variance for these two scales. Cosgrove et al. (2011) found that "small-scale" electric-field variance is roughly 20% as large as the squared mean field, while "resolved-scale" variance is roughly 50% as large as the squared mean field. The contribution of electric-field variance to total Joule heating and its thermosphere/ionosphere effects can be substantial (e.g., Fuller-Rowell et al., 2000; Rodger et al., 2001; Codrescu et al., 2008; Matsuo & Richmond, 2008; Deng et al., 2009).

5 Conductivity relation to electric field

When modeling Joule heating from measured or modeled electric fields or currents together with modeled conductivities, it is important to have the spatial structures of the electric fields and conductivities properly matched. There can exist spatial/temporal correlations between the electric field and conductivity that affect the calculation of total Joule heating. From an analysis of EISCAT electric field and conductance measurements around the March equinox, Aikio and Selkälä (2009) found that the Pedersen conductance can be either positively or negatively correlated with the electric-field strength, depending on MLT and K_p level, and that this correlation affects the calculation of Joule heating. Cosgrove et al. (2011) similarly found both positive and negative correlations between the conductance and electric-field strength in their analysis of Sondrestrom radar data. Based on analysis of spacecraft data, Q. Zhu et al. (2018) quantified how positive and negative correlations between small- and meso-scale structures in electric fields and auroral electron precipitation affect height-integrated Joule heating.

As noted by Milikh et al. (2006) and Dimant and Oppenheim (2011b), modeling of conductivities in the E region can also be affected by electron temperature increases due to Farley-Buneman turbulence, owing to the inverse dependence of the ion-electron recombination rate on electron temperature (Schlegel, 1982). In the F region the conductivity can be reduced by strong electric fields that heat the ions and increase their loss rate (Schunk et al., 1976). Meridional $\mathbf{E} \times \mathbf{B}$ drifts have an upward or downward component that raise or lower the F region. This decreases or increases the height-integrated F-region conductivity, which is proportional to the neutral density that decreases with increasing height.

6 Poynting flux

There is a way to estimate height-integrated Joule heating from spacecraft observations that circumvents problems in estimating ionospheric conductivities and the effects of plasma irregularities. Kelley et al. (1991) pointed out how measurements of the electric and magnetic fields above the ionosphere can be used to determine the downward component of the Poynting vector, or Poynting flux, and to estimate the height-integrated energy dissipation in the ionosphere/thermosphere by application of Poynting's Theorem (Poynting, 1884). As discussed by Kelley et al. (1991), Thayer and Semeter (2004), and others, it is useful for many ionospheric purposes to use the perturbation Poynting vector

$$\mathbf{S}_p = \mathbf{E} \times \delta\mathbf{B}/\mu_0 \tag{5}$$

where $\delta\mathbf{B}$ is the perturbation of the geomagnetic field with respect to the main field $\mathbf{B}_0$, and μ_0 is the permeability of free space. If the electric field is electrostatic, the horizontally integrated perturbation Poynting flux over the top of the ionosphere essentially equals the volume-integrated electromagnetic energy dissipation within the ionosphere. Energy transfer associated with non-electrostatic electric fields, such as ULF waves, is usually much smaller than that associated with quasi-static fields (Hartinger et al., 2015). Models of ionosphere-thermosphere dynamics show that the horizontally integrated energy flux is close to the total Joule heating (e.g., G. Lu et al., 1995; Matsuo & Richmond, 2008), with a minor contribution going to net generation of total kinetic energy of the wind, even though locally the transfer of electromagnetic energy to or from the wind ($\mathbf{V}_n \cdot \mathbf{J} \times \mathbf{B}$) can be large (e.g. Thayer, 1998; Hurd & Larsen, 2016).

Under idealized conditions where $\mathbf{E}$ is orthogonal to the component of $\delta\mathbf{B}$ transverse to $\mathbf{B}_0$ and the two are proportional to each other over the top of the ionosphere, a point measurement of perturbation Poynting flux above the ionosphere gives the height-integrated rate of electromagnetic energy dissipation in the column below (Kelley et al., 1991; Waters et al., 2004; C. Huang & Burke, 2004; Weimer, 2005; Richmond, 2010). In more general cases Richmond (2010) showed that the integrated Poynting flux over an area above the ionosphere bounded by an equipotential equals the electromagnetic energy dissipation rate in the volume below bounded by that equipotential on the sides and by the base of the ionosphere at the bottom, calling this the Equipotential-Boundary Poynting-Flux (EBPF) Theorem. The EBPF Theorem can be applied separately to different components of the electric potential, such as the large- and small-scale components. Since contours of the small-scale component of potential above the ionosphere tend to close over relatively localized regions, the associated small-scale structures of perturbation Poynting flux tend to be dissipated locally along geomagnetic-field lines below. However, for large-scale structures of perturbation Poynting flux the local Poynting flux does not necessarily equal the height-integrated energy dissipation below, as also shown by Vanhamäki et al. (2012). In practice, this means that Poynting-flux measurements over regions of low ionospheric conductivity may differ significantly from the local rate of height-integrated energy dissipation, and that measurements of upward Poynting flux (e.g., Kelley et al., 1991; Gary et al., 1994, 1995) may not necessarily coincide with regions where the ionospheric wind dynamo is a net generator of electromagnetic energy.

7 Observations and modeling of Joule heating and Poynting flux

Joule heating can be calculated from (1) or (3) if all the parameters are known through adequate measurements or models. On the other hand, Poynting flux provides energy input estimates only in a height-integrated sense, and so certain assumptions have to be made to be able to use Poynting flux in models of upper-atmosphere response (Deng et al., 2009). The heating rate can also be estimated from measurements of the ion and electron temperatures (e.g., St. Maurice & Hanson, 1982; St. Maurice et al., 1999). Measurements are available only at very limited locations and times, and so for applications requiring global knowledge of the heating, information from empirical models is generally required. Incoherent-scatter radars have provided detailed information about the vertical and temporal structure of overhead Joule heating (e.g. Wickwar et al., 1974; Banks, 1977; Vickrey et al., 1982; Thayer, 1998, 2000; Fujii et al., 1999; Aikio & Selkälä, 2009; Cai et al., 2013).

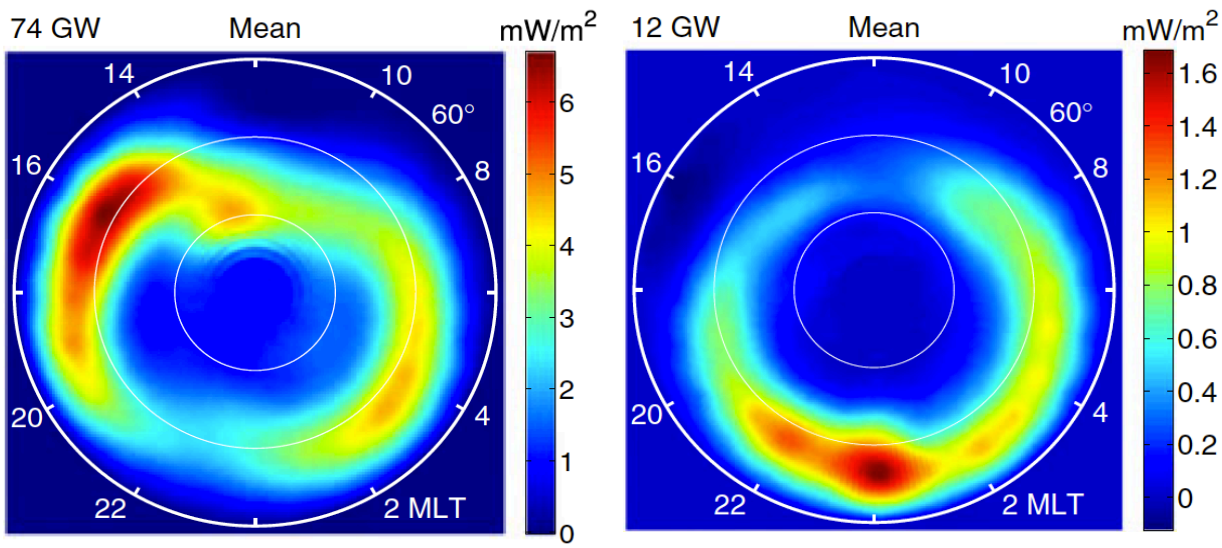

Figure 1. (Left) Average of the 30 sample distributions, covering all seasons and geophysical conditions, used for constructing the Poynting flux model. The hemispherically integrated flux is 74 GW. (Right) Average of the 30 sample distributions, covering all seasons and geophysical conditions, used for constructing the kinetic energy flux model. The hemispherically integrated flux is 12 GW. Note the different color scales on the left and right. [Source: Cosgrove et al., 2014, adapted from (left) figure 2, p. 418 and (right) figure 14, p. 427. Reproduced with permission of the American Geophysical Union.]

Cosgrove et al. (2014) constructed an empirical model of Poynting flux over the polar region as a function of magnetic latitude, MLT, dipole tilt angle, the IMF B_y and B_z components, and the *AL* index, using an extensive data base from the FAST spacecraft. As explained earlier, the Poynting flux usually gives a good indication of height-integrated Joule heating, although it does not precisely locate the energy input. Figure 1 shows the distributions of Poynting flux and energy flux of precipitating auroral electrons averaged for all conditions (season, IMF strength and direction). The largest Poynting fluxes encompass the polar cap, with a maximum in the afternoon and minima around 10 MLT and 23 MLT. There are secondary maxima around 3 MLT at 70° magnetic latitude and shortly after 12 MLT at 78° magnetic latitude, in the so-called cusp region. Strong Poynting flux or Joule heating in the cusp region has also been shown in other studies (Foster et al., 1983; Rich et al., 1991; Gary et al., 1995; Olsson et al., 2004; McHarg et al., 2005; Knipp et al., 2011; Wilder et al., 2012; Y. Lu et al., 2018), while Cai et al. (2016) found there is often a "hot spot" at 75° magnetic latitude around 14-15 MLT. The cusp maximum appears most strongly when the IMF has a northward component, and is the dominant feature when the IMF clock angle is close to 0°. Figure 2 shows how the integral of the Poynting flux over the polar region varies with IMF clock angle and magnitude, dipole tilt angle (positive values representing summer conditions), and the magnitude of the *AL* index.

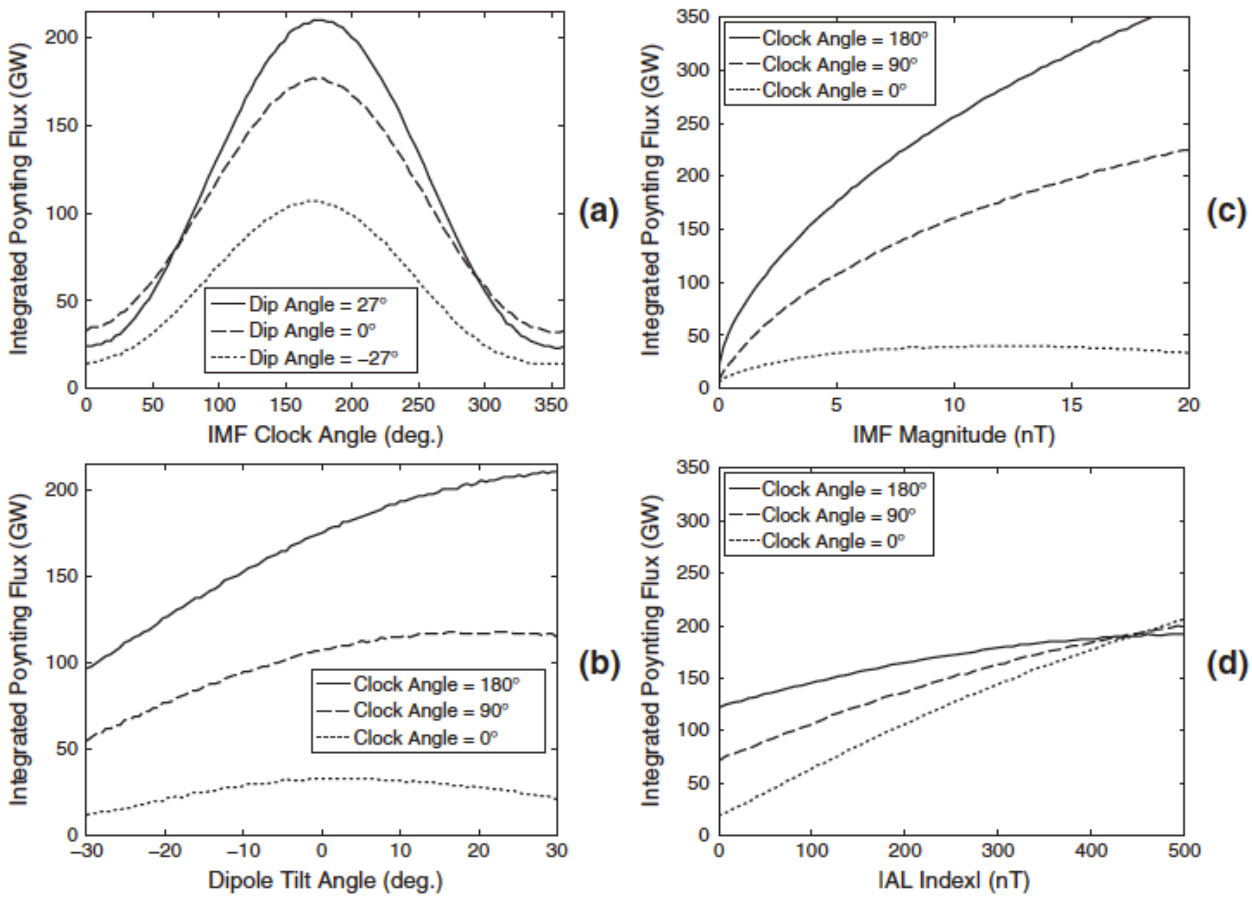

Figure 2. Plots of the integrated Poynting flux as a function of various parameters. (a) The dependence on the IMF clock angle. (b) The dependence on the magnetic dipole tilt angle. (c) The dependence on the IMF magnitude in the GSM *y-z* plane. (d) The dependence on the *AL* index. Note the apparent saturation of the Poynting flux for large (negative) *AL* index, which behavior is probably nonphysical. When not otherwise indicated, the magnetic dipole tilt angle is 0°, the solar wind velocity is 450 km/s, the solar wind number density is 4 cm^{-3}, and the IMF strength in the GSM *y-z* plane is 5 nT. [Source: Cosgrove et al., 2014, figure 6, p. 422. Reproduced with permission of the American Geophysical Union.]

8 Estimating Joule heating through data assimilation

Empirical models are very useful for understanding how Joule heating varies with location, time, and season, and how it depends on external variations in solar and magnetic activity and conditions in the solar wind. Such models are often sufficient to characterize magnetospheric energy inputs to the upper atmosphere for climatological studies of the upper atmosphere and for general responses to events like geomagnetic storms. However, because observations show that the energy inputs are highly variable in time and space, especially during storms but also during non-storm conditions in regions like the dayside cusp, modeling thermospheric responses to Joule heating more accurately requires more detailed information about the energy inputs in time and space for such events. An approach to determining the space-time variations of magnetospheric energy inputs for individual events is through data assimilation. A simple form of data assimilation is to use a distribution of observations related to high-latitude electric fields and currents to produce a map of those fields and currents over the polar regions. Kamide et al. (1981) did this using ground magnetometer data to produce a map of ionospheric equivalent current, then to solve for an electric potential that drives the equivalent current using an ionospheric conductance model. Richmond and Kamide (1988) and Richmond et al. (1988) advanced the mapping of ionospheric electrodynamics by applying data-assimilation tools to combine ground-magnetometer data with climatological models of conductance and electric potential as well as radar observations of ionospheric drifts in order to constrain the estimated maps of electrodynamic features in an optimal manner, given certain assumptions about conductances, thermospheric winds, and current geometry. The procedure was later named Assimilative Mapping of Ionospheric Electrodynamics (AMIE) (Richmond, 1992). It provides estimates of the large-scale electric fields, conductivities, and currents, as well as estimates of the uncertainty in these estimates. A quantitative estimate of the electric-field uncertainty can be used to correct estimates of Joule heating owing to underestimation of the squared electric-field strength (Richmond et al., 1990; G. Lu et al., 1998). AMIE has been extensively used to estimate energy and momentum inputs to the upper atmosphere during disturbed periods (e.g., G. Lu et al., 1995, 1998, 2014, 2016; Emery et al., 1996; Wilder et al., 2012). Matsuo et al. (2005) showed how the AMIE procedure could be improved by dynamic fitting of covariance matrix functions to the data. Assimilative mapping procedures for SuperDARN data have been developed by Ruohoniemi and Baker (1998), Shepherd and Ruohoniemi (2000), Cousins et al. (2013), and Gjerloev et al. (2018), while Waters et al. (2001), Anderson et al. (2014), Cousins et al. (2015), and Matsuo et al. (2015) developed procedures for mapping electrodynamic patterns using multi-satellite magnetometer measurements of magnetic perturbations above the ionosphere.

The data-assimilation procedures for high-latitude electrodynamics developed so far have made simplifying assumptions about the conductivities and winds, with the winds generally neglected altogether. This limitation, as well as the inherent errors in the estimated fields, give rise to substantial uncertainty in the Joule heating and the thermosphere/ionosphere responses (e.g., Pedatella et al., 2018). More-accurate data assimilation could potentially be achieved by directly assimilating the various observations into a dynamic model of the thermosphere and ionosphere, taking into account the effects of electric fields on electric conductivities and neutral winds.

9 Dynamical effects of Joule heating

Rapid variations of the heating produce thermospheric gravity waves in the lower thermosphere that propagate globally into the upper thermosphere, causing large oscillations of wind, temperature, composition, and density as well as large-scale traveling ionospheric disturbances (e.g., Wright, 1960; Chimonas & Hines, 1970; Testud, 1970; Yeh & Liu, 1974; Richmond & Matsushita, 1988; Mayr et al., 1990; Fuller-Rowell et al., 1999; Forbes et al., 2005; Bruinsma et al., 2006; Bruinsma & Forbes, 2010; G. Lu et al., 2016). Figure 3 shows height-time variations of a number of thermosphere/ionosphere quantities as observed and simulated above the locations of the Millstone Hill (42.6°N and 288.5°E) and Arecibo (18.3°N and 293.3°E) radars for a magnetic storm on 2005 September 10 (G. Lu et al., 2008). A pulse of equatorward wind arrives at Millstone Hill starting around 16.7 UT, and at Arecibo starting around 17.8 UT. The wind pulse maximizes at later times with descending altitude. It causes the ionosphere to rise temporarily, and then fall, as the gravity wave passes.

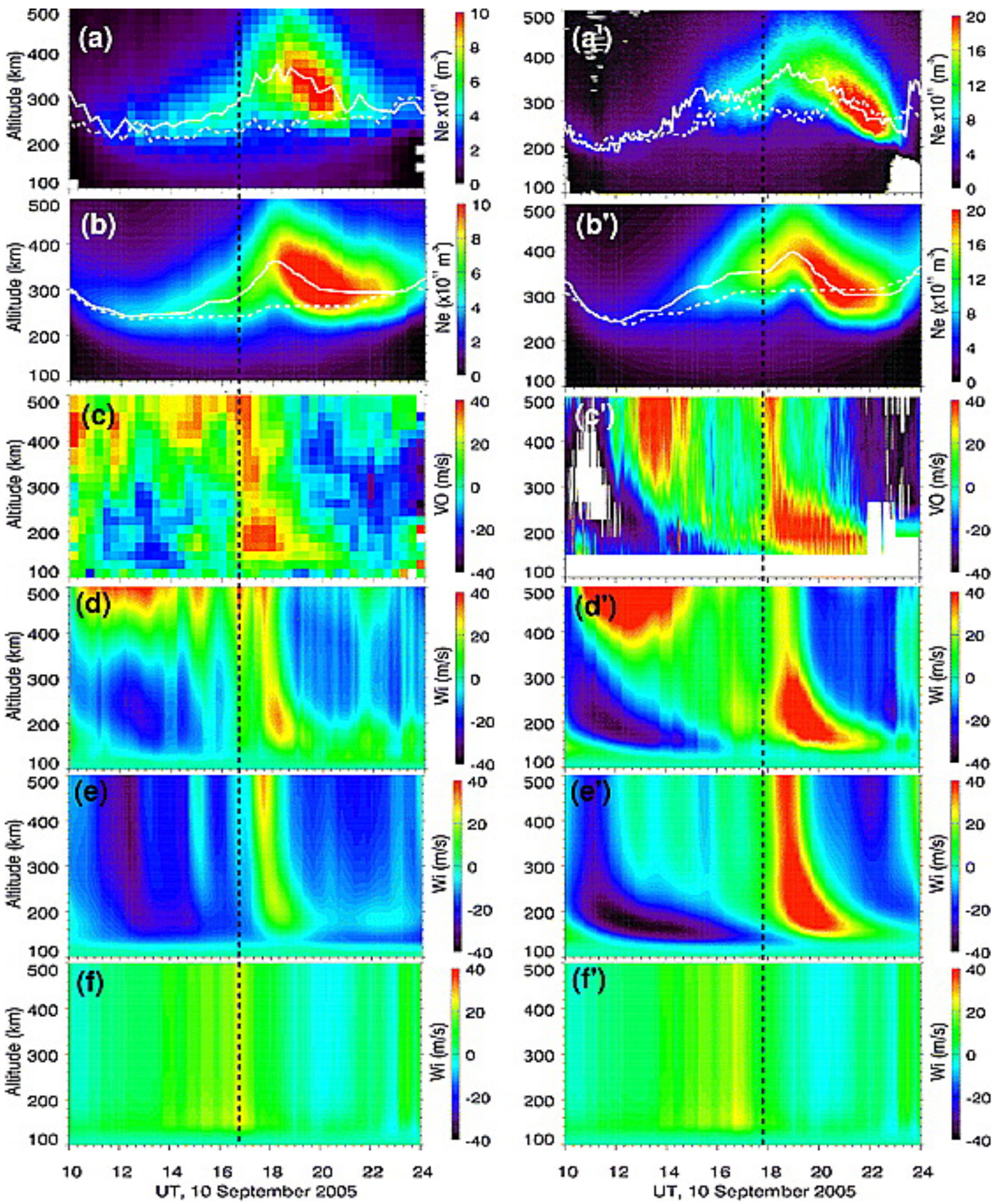

Figure 3. UT versus altitude profiles of (first row) measured electron density, (second row) simulated electron density, (third row) measured vertical ion drift, (fourth row) simulated vertical ion drift, (fifth row) simulated vertical ion drift due to neutral wind, (sixth row) and the

simulated vertical ion drift component due to electric field. The solid white lines show the (first row) observed and (second row) simulated h_mF_2 on the storm day of 10 September, and the dashed white lines indicate the corresponding h_mF_2 on the quiet day of 8 September. The vertical dashed lines mark the onset of upward lift of electron density peak height over (left column) Millstone Hill and (right column) Arecibo. [Source: Lu et al., 2008, figure 2, p. A08304(3). Reproduced with permission of the American Geophysical Union.]

Joule heating of a thermospheric gas parcel causes it to expand and to be more buoyant than its surroundings, which induces it to rise. Vertical winds are produced, which couple with horizontal outflow at higher altitudes, inflow at lower altitudes, and subsidence at other latitudes. On a global scale, circulation changes propagate at speeds up to the limiting horizontal speed of gravity waves, nearly the speed of sound. Thus within several hours the entire Earth responds to changes of Joule heating at high latitudes (e.g., Volland & Mayr, 1971; Mayr & Volland, 1973; Richmond, 1979; Fuller-Rowell et al., 1994, 1997; Sutton et al., 2009). The outflow and inflow can lie several scale heights apart in the vertical. Because the outflow and inflow mass fluxes must balance, the outflow in the low-density region has a much larger velocity than the inflow in the high-density region.

As a heated air parcel rises, it expands and cools adiabatically. In fact, there is a tendency for the parcel to move upward at such a rate that its density remains similar to that of its surroundings, thereby tending to eliminate horizontal variations of pressure and pressure scale height (Hays et al., 1973). Only relatively small horizontal pressure gradients are needed to drive the divergent horizontal winds that balance the mass convergence associated with the upward wind. However, horizontal gradients of the scale height are not completely eliminated, for at least three reasons. First, transience in the dynamics, especially due to gravity waves, is inherently associated with pressure gradients. Second, even in a steady state, residual horizontal pressure gradients are needed to balance other forces like the Coriolis and centrifugal forces and the forces due to ion drag and viscosity (Schoendorf et al., 1996; Fuller-Rowell et al., 1999; G. Lu et al., 2016). In most cases these forces have little direct relation to Joule heating, and so the horizontal pressure variations and related temperature and density variations can have patterns very different from those of Joule heating (Mayr & Harris, 1978; Trinks et al., 1978; Schoendorf et al., 1996; G. Lu et al., 2016). Third, rapid heat conduction and vertical diffusion in the upper thermosphere tend to keep the upper thermosphere close to a state of isothermal diffusive equilibrium, in which the density variation with height would be entirely determined by the temperature and composition at the lowest altitude where isothermal diffusive equilibrium is effective. The pressure scale height is proportional to T/m, where T is temperature and m is the mean molecular mass. For a state of isothermal diffusive equilibrium T would be constant in height but m would decrease with increasing height at a rate dependent on the O/N_2 ratio. Even if the pressure scale height at 400 km were horizontally uniform but T and m each varied horizontally, T/m would not be horizontally uniform at other heights. The study by Thayer et al. (2012) explains how the scale heights of pressure and density differ, depending on different thermospheric compositions.

10 Joule heating effects on composition, temperature, and density

Since the O/N_2 ratio in the thermosphere increases with altitude, an air parcel rising from lower to higher altitudes has a smaller O/N_2 ratio than its surroundings, which means its mean molecular mass is greater than that of its surroundings. In the upper thermosphere regions of enhanced N_2 density are indicative of strong heating below (Taeusch et al., 1971; Taeusch & Hinton, 1975). If the circulation were able to completely eliminate horizontal variations of T/m, regions of enhanced m produced by upwelling would coincide with regions of proportionately enhanced temperature. As shown by Mayr and Volland (1973), the high-latitude decrease of O/N_2, which increases m, allows the temperature to increase considerably above the temperature in neighboring regions with smaller O/N_2 density. Other observations and model studies also indicate that T and m in the upper thermosphere tend to be spatially correlated over the Earth during disturbances (e.g., Qian et al., 2010; G. Lu et al., 2016).

Most of the Joule heating occurs in the lower thermosphere, where Pedersen conductivity is greatest when there is ionization by sunlight or auroral particle precipitation. Only 18-34% of the Joule heating occurs above 150 km (Deng et al., 2011a; Y. Huang et al., 2012b). However, owing to the smaller mass density at high altitudes, this relatively small high-altitude fraction of the heating has a disproportionate impact on the upper thermosphere and F-region ionosphere (Deng et al., 2011a; Y. Huang et al., 2012b; Brinkman et al., 2016). The immediate temperature response to a change in heating per unit volume is inversely proportional to the mass density, which is roughly a thousand times smaller at 400 km than at 125 km. However, temperature perturbations at high altitude are smoothed by rapid heat conduction, which is also inversely proportional to air density, so that after 6 hours most of the heat deposited anywhere above 150 km has spread out over all altitudes above 150 km, with some of the heat conducted down below 150 km. The thermospheric density at 400 km responds to changes in scale height at all lower altitudes, so on a global scale Joule heat deposited anywhere above 150 km affects the 400 km density comparably after about 6 hours. On the other hand, heat deposited below 150 km has a much smaller effect on the density at 400 km within 6 hours, apart from the possible generation of acoustic-gravity waves (Deng et al., 2011a). However, the low-altitude heat plays an important role in high-altitude density changes on longer time scales. Y. Huang et al. (2012b) analyzed the effects of heating at different heights on the global 400 km density response.

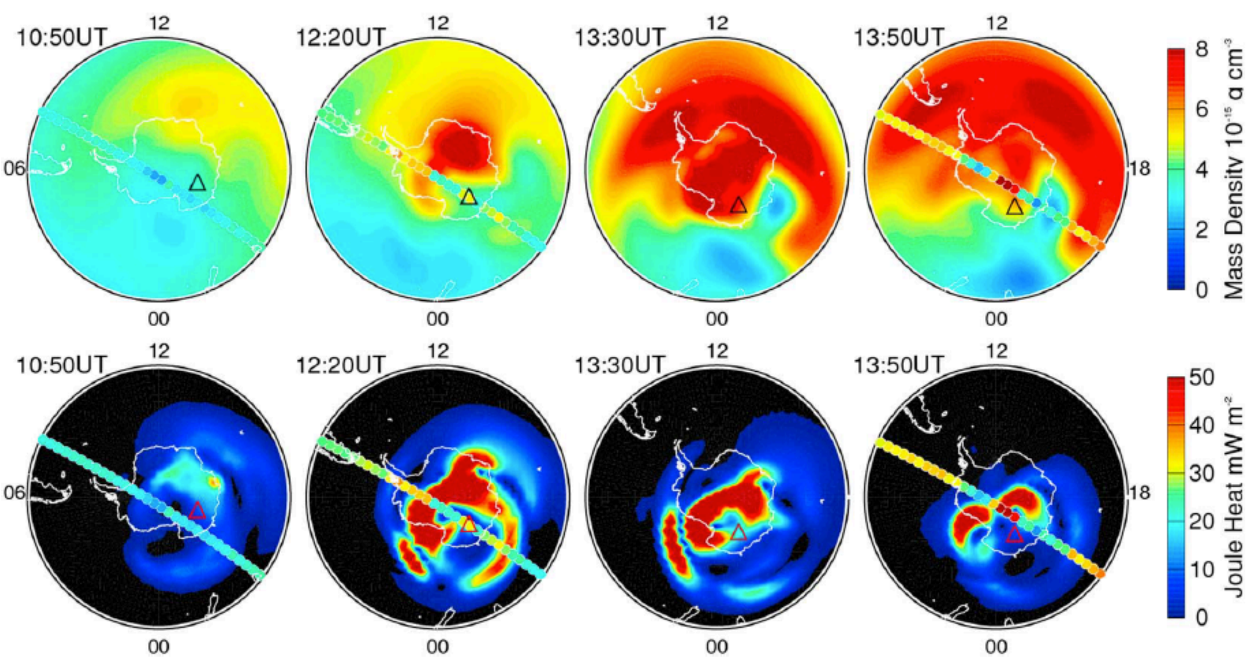

Figure 4. Maps of (top row) neutral mass density at 380 km and (bottom row) height-integrated Joule heating over the southern hemisphere. The small colored dots indicate the CHAMP trajectory, with the color of each dot corresponding to the mass density value measured by CHAMP using the color scale from the top row. The outer circle corresponds to 40ºS, and the triangle in each map indicates the magnetic south pole. [Source: G. Lu et al., 2016, figure 4, p. 7115. Reproduced with permission of the American Geophysical Union.]

An example of a model simulation of the complex relation between upper-thermosphere density and Joule heating is illustrated in Figure 4. This shows sequences of neutral mass density at 380 km altitude (top) and height-integrated Joule heating (bottom) over the southern polar region (-40° to -90° geographic latitude) for the geomagnetic storm of 2005 January 17, with observed mass densities from the CHAMP satellite overlain. There are density increases over Antarctica at 12:20 UT and 13:30 UT that have some correspondence with the distributions of Joule heating at those times, though many details differ. At 13:50 UT the spatial correspondence between density and height-integrated Joule heating has disappeared entirely, owing to the relaxation of the polar density bulge and the equatorward propagation of a large-scale gravity wave.

It is clear that Joule heating has a major impact on the thermosphere during magnetic storms. Even at quiet times high-latitude Joule heating affects thermospheric temperature, composition, and density not only locally, but to some extent globally (Reber & Hedin, 1974; Dickinson et al., 1975, 1977; Roble et al., 1977). Knipp et al. (2004) estimated that daily-average Joule heating, integrated over the globe, ranged from 7 GW to 2035 GW during the years 1975-2003, with an average value of 95 GW. This amounts to 16% of the average total energy input to the thermosphere, 595 GW, from combined solar extreme- and far-ultraviolet radiation, Joule heating, and auroral particle precipitation. When we take into account that less than half of the solar radiation and auroral particle energy absorbed in the thermosphere leads to direct heating (the remainder going to the breaking of O_2 chemical bonds and to airglow), the relative importance of Joule heating to overall thermospheric heating is seen to be quite important. During large magnetic storms Joule heating can totally dominate thermospheric heat input.

Joule heating also affects thermospheric temperature indirectly, through its role in modulating the production of radiatively active NO. Because the reaction rate of ground-state N with O_2 to form NO is highly dependent on temperature (Siskind et al., 1989), more NO is produced when the temperature is elevated. The increased NO density, in turn, increases the radiative cooling rate of the thermosphere (Barth et al., 2009).

Studies of how the thermosphere responds to recurrent geomagnetic activity have helped quantify the role of Joule heating (e.g., Mlynczak et al., 2008; Deng et al., 2011b; Y. Huang et al., 2012a; Jiang et al., 2014). For example, Jiang et al. (2014) showed that the standard parameterization of high-latitude electric potential and particle precipitation used in the Thermosphere-Ionosphere-Mesosphere General Circulation Model (TIME-GCM) based on the K_p index underestimate the amount of Joule heating needed to explain observed 9-day and 13.5-day periodicities in upper-thermospheric density associated with recurrent geomagnetic activity, and they suggested that additional heating associated with electric-field variability might explain the underestimation. The results of Y. Huang et al. (2012a) support this explanation, by showing that Joule heating estimations that use the variable electric fields provided by AMIE data assimilation produce about 2.5 times as much heating as an empirical model of high-latitude fields.

11 Summary

The main points of this paper can be summarized as follows.

- Joule heating is an important energy source driving thermospheric temperature, circulation, composition, and density. Its effects are particularly strong during magnetic storms, but it contributes to global thermospheric structure even at magnetically quiet times.
- For a given electric field and conductivity, winds either increase or decrease Joule heating, depending on direction and temporal variability.
- Plasma turbulence generated by strong electric fields can greatly increase small-scale electric fields and increase Joule heating and the electron temperature.
- Electric-field structures with scale sizes of roughly 1 km to 300 km can make a comparable contribution to Joule heating as the large-scale field. Variability of the large-scale field about the climatological average also affects the calculation of Joule heating.
- Joule heating is affected by spatial/temporal correlations between the electric field and conductivity, which can be positive or negative. The conductivity can be affected by electric fields through changes in electron and ion temperature that affect ion loss rates, and also through vertical displacement of F-region plasma.
- Estimates of height-integrated Joule heating can be obtained from the field-aligned Poynting flux measured above the ionosphere, although the estimates can mislocate the precise region of energy deposition.
- Studies of Joule heating by incoherent-scatter radar have shown complex height and time structures.
- Analyses of downward Poynting flux above the ionosphere have established that most energy is deposited near the morning and afternoon/evening sides of the auroral oval, often with a substantial additional contribution in the magnetospheric cusp region.
- Data assimilation using multiple observations of ion velocities and magnetic perturbations on the ground and in space can help quantify complex spatial/temporal variations of Joule heating.
- Rapid changes of Joule heating launch gravity waves from the lower thermosphere that propagate globally into the upper thermosphere.
- High-latitude Joule heating drives upward winds that induce a global circulation with large equatorward winds at altitudes above the altitude of the main heating region and small poleward winds at altitudes below this region, with subsidence at middle and low latitudes. The circulation is established on a time scale of several hours, in conjunction with the global propagation of gravity waves.
- The circulation acts to reduce horizontal variations of the pressure scale height, although some horizontal pressure gradients persist owing to gravity waves and the tendency of horizontal pressure gradients to balance Coriolis, centrifugal, ion-drag, and viscous forces on a time scale of hours.
- Because of complex factors affecting the pressure that are only indirectly related to Joule heating, the distributions of temperature and density in the upper thermosphere often show little relation to the distribution of Joule heating.
- Vertical winds alter the thermospheric composition, decreasing the O/N_2 ratio in regions of heating and increasing the ratio in regions of subsidence. Horizontal transport of air parcels with enhanced or reduced O/N_2 ratio by the circulation occurs much more slowly than the gravity-wave propagation speed.

• The tendency of the circulation to reduce horizontal variations of the scale height produces spatial correlation between the temperature and the mean molecular mass in the upper thermosphere on a time scale of hours.
• The upper thermosphere is affected more by the fraction of Joule heating deposited above 150 km, in the F region, than by the larger amount of Joule heating deposited below 150 km, in the E region. The horizontal distributions of E- and F-region heating can be quite different.
• Storm-time increases of temperature cause increases in NO density, which increases the rate of infrared cooling of the thermosphere.
• Studies of the thermospheric response to recurrent geomagnetic activity have helped quantify the relation of Joule heating to geomagnetic activity.

Acknowledgments

This work was supported by NASA grant 80NSSC17K0719 and AFOSR grant FA9550-17-1-0248. The National Center for Atmospheric Research is sponsored by the National Science Foundation.

References

Aikio, A.T., & Selkälä, A. (2009), Statistical properties of Joule heating rate, electric field and conductances at high latitudes, *Annales Geophysicae*, 27, 2661-2673, www.anngeophys.net/27/2661/2009/

Aikio, A.T., Cai, L., & Nygrén, T. (2012), Statistical distribution of height-integrated energy exchange rates in the ionosphere, *Journal of Geophysical Research*, 117, A10325, doi:10.1029/2012JA018078

Anderson, B.J., Korth, H., Waters, C.L., Green, D.L, Merkin, V.G., Barnes, R.J., & Dyrud, L.P. (2014), Development of large-scale Birkeland currents determined from the Active Magnetosphere and Planetary Electrodynamics Response Experiment, *Geophysical Research Letters,* 41, 3017-3025, doi:10.1002/2014GL059941

Axford, W.I., & Hines, C.O. (1961), A unifying theory of high-latitude geophysical phenomena and geomagnetic storms, *Canadian Journal of Physics*, 39, 1433-1464.

Bahcivan, H. (2007), Plasma wave heating during extreme electric fields in the high-latitude E region, *Geophysical Research Letters,* 34, L15106, doi:10.1029/2006GL029236

Banks, P.M. (1977), Observations of joule and particle heating in the auroral zone, *Journal of Atmospheric and Terrestrial Physics,* 39, 179-193.

Barth, C.A., Lu, G., & Roble, R.G. (2009), Joule heating and nitric oxide in the thermosphere, *Journal of Geophysical Research*, 114, A05301, doi:10.1029/2008JA013765

Billett, D.D., Grocott, A., Wild, J.A., Walach, M.-T., & Kosch, M.J. (2018). Diurnal variations in global Joule heating morphology and magnitude due to neutral winds. *Journal of Geophysical Research: Space Physics,* 123, 2398-2411. https://doi.org/10.1002/2017JA025141

Brekke, A., & Kamide, Y. (1996), On the relationship between joule and frictional heating in the polar ionosphere, *Journal of Atmospheric and Terrestrial Physics,* 58, 139-143, https://doi.org/10.1016/0021-9169(95)00025-9

Brekke, A., & Rino, C.L. (1978), High-resolution altitude profiles of the auroral zone energy dissipation due to ionospheric currents, *Journal of Geophysical Research*, 83(A6), 2517-2524.

Brinkman, D.G., Walterscheid, R.L., Clemmons, J.H., & Hecht, J.H. (2016), High-resolution modeling of the cusp density anomaly: Response to particle and Joule heating under typical conditions, *Journal of Geophysical Research: Space Physics,* 121, 2645-2661, doi:10.1002/2015JA021658

Bruinsma, S., Forbes, J.M., Nerem, R.S., & Zhang, X. (2006), Thermosphere density response to the 20-21 November 2003 solar and geomagnetic storm from CHAMP and GRACE accelerometer data, *Journal of Geophysical Research*, 111, A06303, doi:10.1029/2005JA011284

Bruinsma, S.L., & Forbes, J.M. (2010), Large-scale traveling atmospheric disturbances (LSTADs) in the thermosphere inferred from CHAMP, GRACE, and SETA accelerometer data, *Journal of Atmospheric and Solar-Terrestrial Physics,* 72, 1057-1066.

Cai, L., Aikio, A.T., & Nygrén, T. (2013), Height-dependent energy exchange rates in the high-latitude E region ionosphere, *Journal of Geophysical Research: Space Physics,* 118, 7369-7383, doi:10.1002/2013JA019195

Cai, L., Aikio, A.T. & Nygrén, T. (2014), Solar wind effect on Joule heating in the high-latitude ionosphere, *Journal of Geophysical Research: Space Physics,* 119, A020269, doi:10.1002/2014JA020269

Cai, L., A.T. Aikio, A.T., & Milan, S.E. (2016), Joule heating hot spot at high latitudes in the afternoon sector, *Journal of Geophysical Research: Space Physics,* 121, 7135-7152, doi:10.1002/2016JA022432

Chimonas, G., & Hines, C.O. (1970), Atmospheric gravity waves launched by auroral currents, *Planetary and Space Science,* 18, 565-582.

Codrescu, M.V., Fuller-Rowell, T.J., & Foster, J.C. (1995), On the importance of E-field variability for Joule heating in the high-latitude thermosphere, *Geophysical Research Letters,* 22, 2393-2396.

Codrescu, M.V., Fuller-Rowell, T.J., Foster, J.C., Holt, J.M., & Cariglia, S.J. (2000), Electric field variability associated with the Millstone Hill electric field model, *Journal of Geophysical Research*, 105, 5265-5273.

Codrescu, M.V., Fuller-Rowell, T.J., Munteanu, V., Minter, C.F., & Millward, G.H. (2008), Validation of the Coupled Thermosphere Ionosphere Plasmasphere Electrodynamics model: CTIPE-Mass Spectrometer Incoherent Scatter temperature comparison, *Space Weather,* 6, S09005, doi:10.1029/2007SW000364

Cole, K.D. (1962), Joule heating of the upper atmosphere, *Australian Journal of Physics*, 15, 223-235.

Cosgrove, R.B., & Thayer, J.P. (2006), Parametric dependence of electric field variability in the Sondrestrom database: A linear relation with Kp, *Journal of Geophysical Research*, 111, A10313, doi:10.1029/2006JA011658

Cosgrove, R.B., & Codrescu, M.V. (2009), Electric field variability and model uncertainty: A classification of source terms in estimating the squared electric field from an electric field model, *Journal of Geophysical Research*, 114, A06301, doi:10.1029/2008JA013929

Cosgrove, R., McCready, M., Tsunoda, R., & Stromme, A. (2011), The bias on the Joule heating estimate: Small-scale variability versus resolved-scale model uncertainty and the correlation of electric field and conductance, *Journal of Geophysical Research*, 116, A09320, doi:10.1029/2011JA016665

Cosgrove, R.B., Bahcivan, H., Chen, S., Strangeway, R.J., Ortega, J., Alhassan, M., Xu, Y., Van Welie, M., Rehberger, J., Musielak, S., & Cahill, N. (2014), Empirical model of Poynting flux derived from FAST data and a cusp signature, *Journal of Geophysical Research: Space Physics,* 119, 411-430, doi:10.1002/2013JA019105

Cousins, E.D.P., Matsuo, T., & Richmond, A.D. (2013), SuperDARN assimilative mapping, *Journal of Geophysical Research: Space Physics,* 118, 7954-7962, doi:10.1002/2013JA019321

Cousins, E.D.P., Matsuo, T., & Richmond, A.D. (2015), Mapping high-latitude ionospheric electrodynamics with SuperDARN and AMPERE, *Journal of Geophysical Research: Space Physics,* 120, 5854-5870, doi:10.1002/2014JA020463

Crowley, G., & Hackert, C.L. (2001), Quantification of high latitude electric field variability, *Geophysical Research Letters,* 28, 2783-2786.

Deng, Y., & Ridley, A.J. (2007). Possible reasons for underestimating Joule heating in global models: E field variability, spatial resolution, and vertical velocity. *Journal of Geophysical Research*, 112, A09308. https://doi.org/10.1029/2006JA012006

Deng, Y., Maute, A. Richmond, A.D., & Roble, R.G. (2009), Impact of electric field variability on Joule heating and thermospheric temperature and density, *Geophysical Research Letters,* 36, L08105, doi:10.1029/2008GL036916

Deng, Y., Fuller-Rowell, T.J., Akmaev, R.A., & Ridley, A.J. (2011a), Impact of the altitudinal Joule heating distribution on the thermosphere, *Journal of Geophysical Research*, 116, A05313, doi:10.1029/2010JA016019

Deng, Y., Y. Huang, Y., Lei, J., Ridley, A.J., Lopez, R., & Thayer, J. (2011b), Energy input into the upper atmosphere associated with high-speed solar wind streams in 2005, *Journal of Geophysical Research*, 116, A05303, doi:10.1029/2010JA016201

Deng, Y., Sheng, C., Tsurutani, B.T., & Mannucci, A.J. (2018), Possible influence of extreme magnetic storms on the thermosphere in the high latitudes, *Space Weather,* 16, 802-813, doi:10.1029/2018SW001847

Dickinson, R.E., Ridley, E.C., & Roble, R.G. (1975), Meridional circulation in the thermosphere, I. Equinox conditions, *Journal of the Atmospheric Sciences,* 32, 1737-1754.

Dickinson, R.E., Ridley, E.C., & Roble, R.G. (1977), Meridional circulation in the thermosphere, II. Solstice conditions, *Journal of the Atmospheric Sciences,* 34, 178-192. https://doi.org/10.1175/1520-0469(1977)034<0178:MCITTI>2.0.CO;2

Dimant, Y.S., & Milikh, G.M. (2003), Model of anomalous electron heating in the E region: 1. Basic theory, *Journal of Geophysical Research*, 108(A9), 1350, doi:10.1029/2002JA009524

Dimant, Y.S., & Oppenheim, M.M. (2011a), Magnetosphere-ionosphere coupling through E region turbulence: 1. Energy budget, *Journal of Geophysical Research*, 116, A09303, doi:10.1029/2011JA016648

Dimant, Y.S., & Oppenheim, M.M. (2011b), Magnetosphere-ionosphere coupling through E region turbulence: 2. Anomalous conductivities and frictional heating, *Journal of Geophysical Research*, 116, A09304, doi:10.1029/2011JA016649

Emery, B.A., Lu, G., Szuszczewicz, E.P., Richmond, A.D., Roble, R.G., Richards, P.G., Miller, K.L., Niciejewski, R., Evans, D.S., Rich, F.J., Denig, W.F., Chenette, D.L., Wilkinson, P., Pulinets, S., O'Loughlin, K.F., Hanbaba, R., Abdu, M., Jiao, P., Igarashi, K., & Reddy, B.M. (1996), Assimilative mapping of ionospheric electrodynamics in the thermosphere-ionosphere general circulation model comparisons with global ionospheric and thermospheric observations during the GEM/SUNDIAL period of March 28-29, 1992, *Journal of Geophysical Research*, 101, 26,681-26,696.

Fedrizzi, M., Fuller-Rowell, T.J., & Codrescu, M.V. (2012), Global Joule heating index derived from thermospheric density physics-based modeling and observations, *Space Weather,* 10, S03001, doi:10.1029/2011SW000724

Forbes, J. M., Lu, G., Bruinsma, S., Nerem, S., & Zhang, X. (2005), Thermosphere density variations due to the 15-24 April 2002 solar events from CHAMP/STAR accelerometer measurements, *Journal of Geophysical Research*, 110, A12S27, doi:10.1029/2004JA010856

Foster, J.C., St.-Maurice, J.-P., & Abreu, V.J. (1983), Joule heating at high latitudes, *Journal of Geophysical Research*, 88, 4885-4896.

Fujii, R., Nozawa, S., Buchert, S.C., & Brekke, A. (1999), Statistical characteristics of electromagnetic energy transfer between the magnetosphere, the ionosphere, and the thermosphere, *Journal of Geophysical Research*, 104, 2357-2365.

Fuller-Rowell, T.J. (2013), Physical characteristics and modeling of Earth's thermosphere. In J. Huba, R. Schunk, G. Khazanov (Eds.), *Modeling the Ionosphere-Thermosphere System*, Geophysical Monograph (Vol. 201), Washington, DC: American Geophysical Union. doi:10.1029/2012GM001329

Fuller-Rowell, T.J., Codrescu, M.V., Moffett, R.J., & Quegan, S. (1994), Response of the thermosphere and ionosphere to geomagnetic storms, *Journal of Geophysical Research*, 99, 3893-3914.

Fuller-Rowell, T.J., Codrescu, M.V., Roble, R.G., & Richmond, A.D. (1997), How does the thermosphere and ionosphere react to a geomagnetic storm? In *Magnetic Storms,* Geophysical Monograph (Vol. 98, pp. 203-225). Washington, DC: American Geophysical Union.

Fuller-Rowell, T.J., Matsuo, T., Codrescu, M.V., & Marcos, F.A. (1999), Modeling thermospheric neutral density waves and holes in response to high latitude forcing, *Advances in Space Research,* 24, 1447-1458. https://doi.org/10.1016/S0273-1177(99)00705-X

Fuller-Rowell, T.J., Codrescu, M.C., & Wilkinson, P. (2000), Quantitative modeling of the ionospheric response to geomagnetic activity, *Annales Geophysicae*, 18, 766-781.

Gary, J.B., Heelis, R.A., Hanson, W.B., & Slavin, J.A. (1994), Field-aligned Poynting flux observations in the high-latitude ionosphere, *Journal of Geophysical Research*, 99, 11417-11427.

Gary, J.B., Heelis, R.A., & Thayer, J.P. (1995), Summary of field-aligned Poynting flux observations from DE2, *Geophysical Research Letters,* 22, 1861-1864.

Gjerloev, J.W., Waters, C.L., & Barnes, R.J. (2018). Deriving global convection maps from SuperDARN measurements. *Journal of Geophysical Research: Space Physics,* 123, 2902-2915. https://doi.org/10.1002/2017JA024543

Hartinger, M.D., Moldwin, M.B., Zou, S., Bonnell, J.W., & Angelopoulos, V. (2015), ULF wave electromagnetic energy flux into the ionosphere: Joule heating implications, *Journal of Geophysical Research: Space Physics,* 120, 494-510, doi:10.1002/2014JA020129

Hays, P.B., Jones, R.A., & Rees, M.H. (1973), Auroral heating and the composition of the neutral atmosphere, *Planetary and Space Science,* 21, 559-573.

Heelis, R.A., & Coley, W.R. (1988), Global and local Joule heating effects seen by DE 2, *Journal of Geophysical Research*, 93, 7551-7557.

Heelis, R.A., & Vickrey, J.F. (1991), Energy dissipation in structured electrodynamic environments, *Journal of Geophysical Research*, 96, 14,189-14,194.

Huang, C.Y., & Burke, W.J. (2004), Transient sheets of field-aligned current observed by DMSP during the main phase of a magnetic superstorm, *Journal of Geophysical Research*, 209, A06303, doi:10.1029/2003JA010067

Huang, Y., Deng, Y., Lei, J., Ridley, A., Lopez, R., Allen, R.C., & Butler, B.M. (2012a), Comparison of Joule heating associated with high-speed solar wind between different models and observations, *Journal of Atmospheric and Solar-Terrestrial Physics,* 75-76, 5-14.

Huang, Y., Richmond, A.D., Deng, Y., & Roble, R. (2012b), Height distribution of Joule heating and its influence on the thermosphere, *Journal of Geophysical Research*, 117, A08334, doi:10.1029/2012JA017885

Hurd, L.D., & Larsen, M.F. (2016), Small-scale fluctuations in barium drifts at high latitudes and associated Joule heating effects, *Journal of Geophysical Research: Space Physics,* 121, 779-789, https://doi.org/10.1002/2015JA021868

Jiang, G., Wang, W., Xu, J., Yue, J., Burns, A.G., Lei, J., Mlynczak, M.G., & Rusell, J.M. III (2014), Responses of the lower thermospheric temperature to the 9 day and 13.5 day oscillations of recurrent geomagnetic activity, *Journal of Geophysical Research: Space Physics,* 119, 4841-4859, doi:10.1002/2013JA019406

Johnson, F.S. (1960), Pressure and temperature equalization at 200-km altitude, *Journal of Geophysical Research*, 65(8), 2227-2232, doi: 10.1029/JZ065i008p02227

Kamide, Y., Richmond, A.D., & Matsushita, S. (1981), Estimation of ionospheric electric fields, ionospheric currents, and field-aligned currents from ground magnetic records, *Journal of Geophysical Research*, 86, 801-813, doi:10.1029/JA086iA02p00801

Kelley, M.C., Knudsen, D.J., & Vickrey, J.F. (1991), Poynting flux measurements on a satellite: a diagnostic tool for space research, *Journal of Geophysical Research*, 96, 201-207.

Knipp, D., Tobiska, W.K., & Emery, B. (2004), Direct and indirect thermospheric heating sources for solar cycles 21-23. *Solar Physics,* 224(1), 495-505. https://doi.org/10.1007/s11207-005-6393-4

Knipp, D., Eriksson, S., Kilcommons, L., Crowley, G., Lei, J., Hairston, M., & Drake, K. (2011), Extreme Poynting flux in the dayside thermosphere: Examples and statistics, *Geophysical Research Letters,* 38, L16102, doi:10.1029/2011GL048302

Lei, J., Thayer, J.P., Burns, A.G., Lu, G., & Deng, Y. (2010), Wind and temperature effects on thermosphere mass density response to the November 2004 geomagnetic storm, *Journal of Geophysical Research*, 115, A05303, doi:10.1029/2009JA014754 Correction: *Journal of Geophysical Research*, 115, A06399, doi:10.1029/2010JA015649

Liu, H., & Lühr, H. (2005), Strong disturbance of the upper thermospheric density due to magnetic storms: CHAMP observations, *Journal of Geophysical Research*, 110, A09S29, doi:10.1029/2004JA010908

Liu, R., Lühr, H., & Ma, S.-Y. (2010), Storm-time related mass density anomalies in the polar cap as observed by CHAMP, *Annales Geophysicae*, 28, 165-180, www.anngeophys.net/28/165/2010/

Lu, G., Richmond, A.D., Emery, B.A., & Roble, R.G. (1995), Magnetosphere-ionosphere-thermosphere coupling: effect of neutral wind on energy transfer and field-aligned current, *Journal of Geophysical Research*, 100, 19,643-19,659.

Lu, G., Baker, D.N., Farrugia, C.J., Lummerzheim, D., Ruohoniemi, J.M., Rich, F.J., Evans, D.S., Lepping, R.P., Brittnacher, M., Li, X., Greenwald, R., Sofko, G., Villain, J., Lester, M., Thayer, J., Moretto, T., Milling, D., Troshichev, O., Zaitzev, A., Makarov, G., & Hayashi, K. (1998), Global energy deposition during the January 1997 magnetic cloud event, *Journal of Geophysical Research*, 103, 11,685-11,694.

Lu, G., Goncharenko, L.P., Richmond, A.D., Roble, R.G., & Aponte, N. (2008), A dayside ionospheric positive storm phase driven by neutral winds, *Journal of Geophysical Research*, 113, A08304, doi:10.1029/2007JA012895

Lu, G., Hagan, M.E., Häusler, K., Doornbos, E., Bruinsma, S., Anderson, B.J., & Korth, H. (2014), Global ionospheric and thermospheric response to the 5 April 2010 geomagnetic storm: An integrated data-model investigation, *Journal of Geophysical Research: Space Physics,* 119, 10,358-10,375, doi:10.1002/2014JA020555

Lu, G., Richmond, A.D., Lühr, H., & Paxton, L. (2016), High-latitude energy input and its impact on the thermosphere, *Journal of Geophysical Research: Space Physics,* 121, 7108-7124, doi:10.1002/2015JA022294

Lu, Y., Deng, Y., Sheng, C., Kilcommons, L., & Knipp, D.J. (2018). Poynting Flux in the Dayside Polar Cap Boundary Regions from DMSP F15 satellite measurements. *Journal of Geophysical Research: Space Physics,* 123, 6948–6956. https://doi.org/10.1029/2018JA025309

Matsuo, T., & Richmond, A.D. (2008), Effects of high-latitude ionospheric electric field variability on global thermospheric Joule heating and mechanical energy transfer rate, *Journal of Geophysical Research*, 113, A07309, doi:10.1029/2007JA012993

Matsuo, T., Richmond, A.D., & Hensel, K. (2003), High-latitude ionospheric electric field variability and electric potential derived from DE-2 plasma drift measurements: Dependence on IMF and dipole tilt, *Journal of Geophysical Research*, 108(A1), 1005, doi:10.1029/2002JA009429

Matsuo, T., Richmond, A.D., & Lu, G. (2005), Optimal interpolation analysis of high-latitude ionospheric electrodynamics using empirical orthogonal functions: Estimation of dominant modes of variability and temporal scales of large-scale electric fields, *Journal of Geophysical Research*, 110, A06301, doi:10.1029/2004JA010531

Matsuo, T., Knipp, D.J., Richmond, A.D., Kilcommons, L., & Anderson, B.J. (2015), Inverse procedure for high-latitude ionospheric electrodynamics: Analysis of satellite-borne magnetometer data. *Journal of Geophysical Research: Space Physics,* 120, 5241-5251. doi:10.1002/2014JA020565

Mayr, H.G., & Harris, I. (1978), Some characteristics of electric field momentum coupling with the neutral atmosphere, *Journal of Geophysical Research*, 83, 3327-3336.

Mayr, H.G., & Volland, H. (1972), Magnetic storm effects in the neutral composition, *Planetary and Space Science,* 20, 379-393.

Mayr, H.G., & Volland, H. (1973), Magnetic storm characteristics of the thermosphere, *Journal of Geophysical Research*, 78, 2251-2264.

Mayr, H.G., Harris, I., & Spencer, N.W. (1978), Some properties of upper atmosphere dynamics, *Reviews of Geophysics*, 16, 539-565.

Mayr, H.G., Harris, I., Herrero, F.A., Spencer, N.W., Varosi, F., & Pesnell, W.D. (1990), Thermospheric gravity waves: observations and interpretation using the transfer function model (TFM), *Space Science Reviews,* 54, 297-375.

McHarg, M., Chun, F., Knipp, D., Lu, G., Emery, B., & Ridley, A. (2005). High-latitude Joule heating response to IMF inputs. *Journal of Geophysical Research*, 110, A08309. https://doi.org/10.1029/2004JA010949

Milikh, G.M., & Dimant, Y.S. (2003), Model of anomalous electron heating in the E region: 2. Detailed numerical modeling, *Journal of Geophysical Research*, 108(A9), 1351, doi:10.1029/2002JA009527

Milikh, G.M., Goncharenko, L.P., Dimant, Y.S., Thayer, J.P., & McCready, M.A. (2006), Anomalous electron heating and its effect on the electron density in the auroral electrojet, *Geophysical Research Letters,* 33, L13809, doi:10.1029/2006GL026530

Mlynczak, M.G., Martin-Torres, F.J., Mertens, C.J., Marshall, B.T., Thompson, R.E., Kozyra, J.U., Remsberg, E.E., Gordley, L.L., Russell, J.M., & Woods, T. (2008), Solar-terrestrial coupling evidenced by periodic behavior in geomagnetic indexes and the infrared energy budget of the thermosphere, *Geophysical Research Letters,* 35, L05808, doi:10.1029/2007GL032620

Olsson, A., Janhunen, P., Karlsson, T., Ivchenko, N., & Blomberg, L.G. (2004), Statistics of Joule heating in the auroral zone and polar cap using Astrid-2 satellite Poynting flux, *Annales Geophysicae*, 22, 4133-4142.

Oppenheim, M.M., Dimant, Y., & Dyrud, L. (2008), Large scale simulations of 2D fully kinetic Farley Buneman turbulence, *Annales Geophysicae*, 26, 543-553, www.anngeophys.net/26/543/2008/

Pedatella, N.M., Lu, G., & Richmond, A.D. (2018), Effects of high-latitude forcing uncertainty on the low-latitude and midlatitude ionosphere. *Journal of Geophysical Research: Space Physics,* 123, 862-882. https://doi.org/10.1002/2017JA024683

Poynting, J.H. (1884), On the transfer of energy in the electromagnetic field, *Philosophical Transactions,* 175, 343-361.

Prölss, G.W. (1980), Magnetic storm associated perturbation of the upper atmosphere: Recent results obtained by satellite-borne gas analyzers, *Reviews of Geophysics,* 18, 183-202.

Prölss, G. (1995), Ionospheric F-region storms, in H. Volland (Ed.) *Handbook of Atmospheric Electrodynamics, Vol. II,* (pp. 195-248). Boca Raton, FL: CRC Press.

Providakes, J.F., Farley, D.T., Fejer, B.G., Sahr, J., Swartz, W.E., Häggström, Å., & Nordling, J.A. (1988), Observations of auroral E region plasma waves and electron heating with EISCAT and a VHF radar interferometer, *Journal of Atmospheric and Terrestrial Physics,* 50, 339-356. https://doi.org/10.1016/0021-9169(88)90019-0

Qian, L., Solomon, S.C., & Mlynczak, M.G. (2010), Model simulation of thermospheric response to recurrent geomagnetic forcing, *Journal of Geophysical Research*, 115, A10301, doi:10.1029/2010JA015309

Reber, C.A., & Hedin, A.E. (1974), Heating of the high-latitude thermosphere during magnetically quiet periods, *Journal of Geophysical Research*, 79, 2457-2461.

Rees, D. (1971), Ionospheric winds in the auroral zone, *Journal of the British Interplanetary Society,* 24, 233-246.

Rees, D. (1995), Observations and modelling of ionospheric and thermospheric disturbances during major geomagnetic storms: a review, *Journal of Atmospheric and Terrestrial Physics,* 57, 1433-1457.

Rees, D., & Fuller-Rowell, T.J. (1989), The response of the thermosphere and ionosphere to magnetospheric forcing, *Philosophical Transactions of the Royal Society of London,* A328, 139-171.

Rees, D., & Fuller-Rowell, T.J. (1991), Thermospheric response and feedback to auroral inputs, In C.-I. Meng, M.J. Rycroft, & L.A. Frank (Eds.), *Auroral Physics* (pp. 51-65). Cambridge, UK: Cambridge University Press.

Rich, F.J., Gussenhoven, M.S., Hardy, D.A., & Holeman, E. (1991), Average height-integrated Joule heating rates and magnetic deflection vectors due to field-aligned currents during sunspot minimum, *Journal of Atmospheric and Terrestrial Physics,* 53, 293-308.

Richmond, A.D. (1979), Thermospheric heating in a magnetic storm: Dynamic transport of energy from high to low latitudes, *Journal of Geophysical Research*, 84, 5259-5266.

Richmond, A.D. (1992), Assimilative mapping of ionospheric electrodynamics, *Advances in Space Research,* 12, (6)59-(6)68.

Richmond, A.D. (2010), On the ionospheric application of Poynting's Theorem, *Journal of Geophysical Research*, 115, A10311, doi:10.1029/2010JA015768

Richmond, A.D., & Kamide, Y. (1988), Mapping electrodynamic features of the high-latitude ionosphere from localized observations: Technique, *Journal of Geophysical Research*, 93, 5741-5759.

Richmond, A.D., & Matsushita, S. (1975), Thermospheric response to a magnetic substorm, *Journal of Geophysical Research*, 80, 2839-2850.

Richmond, A.D., Kamide, Y., Ahn, B.-H., Akasofu, S.I., Alcaydé, D., Blanc, M., de la Beaujardière, O., Evans, D.S., Foster, J.C., Friis-Christensen, E., Fuller-Rowell, T.J., Holt, J.M., Knipp, D., Kroehl, H.W., Lepping, R.P., Pellinen, R.J., Senior, C., & Zaitzev, A.N. (1988), Mapping electrodynamic features of the high-latitude ionosphere from localized observations: Combined incoherent-scatter radar and magnetometer measurements for 1984 January 18-19, *Journal of Geophysical Research*, 93, 5760-5776.

Richmond, A.D., Kamide, Y., Akasofu, S.-I., Alcaydé, D., Blanc, M., de la Beaujardière, O., Evans, D.S., Foster, J.C., Friis-Christensen, E., Holt, J.M., Pellinen, R.J., Senior, C., & Zaitzev, A.N. (1990), Global measures of ionospheric electrodynamic activity inferred from combined incoherent scatter radar and ground magnetometer observations, *Journal of Geophysical Research*, 95, 1061-1071.

Rishbeth, H. (1991), F-region storms and thermospheric dynamics, *Journal of Geomagnetism and Geoelectricity,* 43, Supplement, 513-524.

Roble, R.G., Dickinson, R.E., & Ridley, E.C. (1977), Seasonal and solar cycle variations of the zonal mean circulation in the thermosphere, *Journal of Geophysical Research*, 82, 5493-5504.

Roble, R.G., Dickinson, R.E., Ridley, E.C., Emery, B.A., Hays, P.B., Killeen, T.L., & Spencer, N.W. (1983), The high latitude circulation and temperature structure of the thermosphere near solstice, *Planetary and Space Science,* 31, 1479-1499.

Rodger, A.S., Wells, G.D., Moffett, R.J., & Bailey, G.J. (2001), The variability of Joule heating, and its effects on the ionosphere and thermosphere, *Annales Geophysicae*, 19, 773-782.

Ruohoniemi, J.M., & Baker, K.B. (1998), Large-scale imaging of high-latitude convection with Super Dual Auroral Radar Network HF radar observations, *Journal of Geophysical Research*, 103, 20,797-20,811.

Schlegel, K. (1982), Reduced effective recombination coefficient in the disturbed polar E-region, *Journal of Atmospheric and Terrestrial Physics,* 44, 183-185.

Schoendorf, J., Crowley, G., & Roble, R.G. (1996), Neutral density cells in the high latitude thermosphere–2. Mechanisms, *Journal of Atmospheric and Solar-Terrestrial Physics,* 58, 1769-1781, doi:10.1016/0021-9169(95)00166-2.

Shepherd, S.G., & Ruohoniemi, J.M. (2000), Electrostatic potential patterns in the high-latitude ionosphere constrained by SuperDARN measurements, *Journal of Geophysical Research*, 105, 23,005-23,124.

Schunk, R.W., Banks, P.M., & Raitt, W.J. (1976), Effects of electric fields and other processes upon the nighttime high-latitude F layer, *Journal of Geophysical Research*, 81, 3271-3282.

Siskind, D.E., Barth, C.A., & Roble, R.G. (1989), The response of thermospheric nitric oxide to an auroral storm: 1. Low and middle latitudes, *Journal of Geophysical Research*, 94(A12), 16,885-16,898.

St.-Maurice, J.-P. (1990), Electron heating by plasma waves in the high latitude E-region and related effects: theory, *Advances in Space Research,* 10(6), 239-249.

St.-Maurice, J.-P., & Hanson, W.B. (1982), Ion frictional heating at high latitudes and its possible use for an in situ determination of neutral thermospheric winds and temperatures, *Journal of Geophysical Research*, 87(A9), 7580-7602, doi:10.1029/JA087iA09p07580

St.-Maurice, J.-P., & Laher, R. (1985), Are observed broadband plasma wave amplitudes large enough to explain the enhanced electron temperatures of the high-latitude E region?, *Journal of Geophysical Research*, 90, 2843-2850, doi:10.1029/JA090iA03p02843.

St.-Maurice, J.-P., Cussenot, C., & Kofman, W. (1999), On the usefulness of E region electron temperatures and lower F region ion temperatures for the extraction of thermospheric parameters: a case study, *Annales Geophysicae*, 17, 1182-1198, doi:10.1007/s00585-999-1182-2.

Strangeway, R.J. (2012), The equivalence of Joule dissipation and frictional heating in the collisional ionosphere, *Journal of Geophysical Research*., 117, A02310, doi:10.1029/2011JA017302.

Sutton, E.K., Forbes, J.M. & Nerem, R.S. (2005), Global thermospheric neutral density and wind response to the severe 2003 geomagnetic storms from CHAMP accelerometer data, *Journal of Geophysical Research*, 110, A09S40, doi:10.1029/2004JA010985.

Sutton, E.K., Forbes, J.M., & Knipp, D.J. (2009), Rapid response of the thermosphere to variations in Joule heating, *Journal of Geophysical Research*, 114, A04319, doi:10.1029/2008JA013667.

Taeusch, D.R., & Hinton, B.B. (1975), Structure of electrodynamic and particle heating in the undisturbed polar thermosphere, *Journal of Geophysical Research*, 80, 4346-4350.

Taeusch, D.R., Carignan, G.R., & Reber, C.A. (1971), Neutral composition variation above 400 kilometers during a magnetic storm, *Journal of Geophysical Research*, 76, 8318-8325.

Testud, J. (1970), Gravity waves generated during magnetic substorms, *Journal of Atmospheric and Terrestrial Physics,* 32, 1793-1805.

Thayer, J.P. (1998). Height-resolved Joule heating rates in the high-latitude E region and the influence of neutral winds. *Journal of Geophysical Research*, 103(A1), 471-487.

Thayer, J.P. (2000), High-latitude currents and their energy exchange with the ionosphere-thermosphere system, *Journal of Geophysical Research*, 105, 23,015-23,024, doi:10.1029/1999JA000409.

Thayer, J.P., & Semeter, J. (2004), The convergence of magnetospheric energy flux in the polar atmosphere, *Journal of Atmospheric and Solar-Terrestrial Physics,* 66, 807-824.

Thayer, J.P., & Vickrey, J.F. (1992), On the contribution of the thermospheric neutral wind to high-latitude energetics, *Geophysical Research Letters,* 19, 265-268.

Thayer, J.P., Vickrey, J.F., Heelis, R.A., & Gary, J.B. (1995), Interpretation and modeling of the high-latitude electromagnetic energy flux, *Journal of Geophysical Research*, 100, 19,715-19,728.

Thayer, J.P., Liu, X., Lei, J., Pilinski, M., & Burns, A.G. (2012), The impact of helium on thermosphere mass density response to geomagnetic activity during the recent solar minimum, *Journal of Geophysical Research*, 117, A07315, doi:10.1029/2012JA017832.

Trinks, H., Mayr, H.G., & Philbrick, C.R. (1978), Momentum source signatures in thermospheric neutral composition, *Journal of Geophysical Research*, 83, 1641-1643.

Vanhamäki, H., Yoshikawa, A., Amm, O., & Fujii, R. (2012), Ionospheric Joule heating and Poynting flux in quasi-static approximation, *Journal of Geophysical Research*, 117, A08327, doi:10.1029/2012JA017841

Vasyliunas, & Song, P. (2005), Meaning of ionospheric Joule heating, *Journal of Geophysical Research*, 110, A02301, doi:10.1029/2004JA010615.

Vickrey, J., Vondrak, R., & Matthews, S. (1982), Energy deposition by precipitating particles and Joule dissipation in the auroral ionosphere, *Journal of Geophysical Research*, 87(A7), 5184-5196.

Volland, H. (1979), magnetospheric electric fields and currents and their influence on large scale thermospheric circulation and composition, *Journal of Atmospheric and Terrestrial Physics,* 41, 853-866.

Volland, H., & Mayr, H.G. (1971), Response of the thermospheric density to auroral heating during geomagnetic disturbances, *Journal of Geophysical Research*, 76(16), 3764-3776, doi:10.1029/JA076i016p03764

Waters, C.L., Anderson, B.J., & Liou, K. (2001), Estimation of global field aligned currents using the Iridium System magnetometer data, *Geophysical Research Letters,* 28, 2165-2168.

Waters, C.L., Anderson, B.J., Greenwald, R.A., Barnes, R.J., & Ruohoniemi, J.M. (2004), High-latitude poynting flux from combined Iridium and SuperDARN data, *Annales Geophysicae*, 22, 2861-2875.

Weimer, D.R. (2001), An improved model of ionospheric electric potentials including substorm perturbations and application to the Geospace Environment Modeling November 24, 1996, event, *Journal of Geophysical Research*, 106, 407-416.

Weimer, D.R. (2005), Improved ionospheric electrodynamic models and application to calculating Joule heating rates, *Journal of Geophysical Research*, 110, A05306, doi:10.1029/2004JA010884.

Wickwar, V.B., Baron, M.J., & Sears, R.D. (1975), Auroral energy input from energetic electrons and Joule heating at Chatanika, *Journal of Geophysical Research*., 80, 4364-4367.

Wilder, F.D., Crowley, G., Anderson, B.J., & Richmond, A.D. (2012), Intense dayside Joule heating during the April 5, 2010 geomagnetic storm recovery phase observed by AMIE and AMPERE, *Journal of Geophysical Research*, 117, A05207, doi:10.1029/2011JA017262

Wright, M.D. (1960), Possible identification of atmospheric waves associated with ionospheric storms, *Nature,* 190, 898-899.

Yeh, K.C., & Liu, C.H. (1974), Acoustic gravity waves in the upper atmosphere, *Reviews of Geophysics and Space Physics,* 12, 193-216.

Zhu, Q., Deng, Y., Richmond, A., & Maute, A. (2018), Small- and meso-scale variabilities in the electric field and particle precipitation and their impacts on Joule heating, *Journal of Geophysical Research: Space Physics,* doi:10.1029/2018JA025771

Zhu, X., Talaat, E.R., Baker, J.B., & Yee, J.-H. (2005), A self-consistent derivation of ion drag and joule heating for atmospheric dynamics in the thermosphere. *Annales Geophysicae,* 23, 3313-3322. https://doi.org/10.5194/angeo-23-3313-2005